Article

Assessing the Stress Induced by Novel Packaging in GaN HEMT Devices via Raman Spectroscopy

Zainab Dahrouch [1,*], Giuliana Malta [1,2], Moreno d'Ambrosio [1,*], Angelo Alberto Messina [2,3], Mattia Musolino [2], Alessandro Sitta [2], Michele Calabretta [2] and Salvatore Patanè [1,*]

[1] Dipartimento di Scienze Matematiche e Informatiche, Scienze Fisiche e Scienze della Terra, University of Messina, Viale F. S. D'Alcontres 31, 98166 Messina, Italy; giuliana.malta@st.com
[2] STMicroelectronics, Stradale Primosole 50, 95125 Catania, Italy; angelo.messina@st.com (A.A.M.); mattia.musolino@st.com (M.M.); alessandro.sitta@st.com (A.S.); michele.calabretta@st.com (M.C.)
[3] CNR Institute for Microelectronics and Microsystems, Strada VIII n. 5, 95121 Catania, Italy
* Correspondence: zainab.dahrouch@studenti.unime.it (Z.D.); moreno.dambrosio@studenti.unime.it (M.d.); salvatore.patane@unime.it (S.P.)

Abstract: Micro-Raman spectroscopy was carried out to evaluate the localized residual stresses in commercial Gallium-Nitride-based devices, specifically, AlGaN/GaN high-electron-mobility Transistors (HEMTs) with a novel packaging design provided by STMicroelectronics S.r.l. (Catania, Italy). The packaging plays a key role in protecting the device core against the external environment, thus minimizing damages caused by mechanical shocks, exposure to light, and contact with chemicals, conjointly achieving an efficient heat dissipation rate. Even though the packaging is a required step for the proper functioning of ready-to-use electronic devices, its application typically may introduce mechanical stress to AlGaN/GaN HEMTs, which can result in various reliability issues. In this paper, we investigate the impact of packaging on residual stress by analyzing the frequency shift of the E2 Raman peak along GaN layers and at the GaN/Si interface. An extensive evaluation was conducted using both a packaged device and a wafer-level device. The correlation between Raman frequency shifts of the E2 mode was accurately quantified, revealing a stress mitigation of approximately 0.1 GPa. This reduction is ascribed to the compressive stress introduced by the packaging, which partially offsets the intrinsic tensile stress of the wafer-level device. The proposed methodology could, in principle, be implemented to improve the development of packaging.

Keywords: AlGaN/GaN high-electron-mobility transistor; micro-Raman spectroscopy; power electronic; packaged device; wafer level

Citation: Dahrouch, Z.; Malta, G.; d'Ambrosio, M.; Messina, A.A.; Musolino, M.; Sitta, A.; Calabretta, M.; Patanè, S. Assessing the Stress Induced by Novel Packaging in GaN HEMT Devices via Raman Spectroscopy. *Appl. Sci.* **2024**, *14*, 4230. https://doi.org/10.3390/app14104230

Academic Editor: Yufei Ma

Received: 17 April 2024
Revised: 9 May 2024
Accepted: 14 May 2024
Published: 16 May 2024

Copyright: © 2024 by the authors. Licensee MDPI, Basel, Switzerland. This article is an open access article distributed under the terms and conditions of the Creative Commons Attribution (CC BY) license (https://creativecommons.org/licenses/by/4.0/).

1. Introduction

Among Wide-Bandgap Semiconductors (WBSs), Gallium Nitride (GaN) is emerging as the latest breakthrough in developing novel energy-efficient power electronic devices and optoelectronic components [1]. It is characterized by a crystallographic arrangement typical of wurtzite, where Gallium (Ga) and Nitrogen (N) atoms are spatially arranged to form a superimposed hexagonal packed lattice. Power electronics has recently leveraged the characteristics of wide-bandgap materials to overcome the limitations imposed by silicon. In particular, the increasing demand for the next generation of high-efficiency power converters has pushed the development of devices capable of operating at higher frequencies and temperatures, achieving higher conversion efficiency. Among these devices, GaN-based technology has been employed to develop AlGaN/GaN high-electron-mobility transistors (HEMTs) [2–4]. These devices find applications in electric vehicles, phone chargers, renewable energies, and more as they meet the above specifications, are able to operate at high temperatures, frequencies, voltages, and currents, and allow the design of systems that occupy less space and generate less heat [5]. However, due to the limited commercial availability of bulk GaN substrates [6], GaN-based electronics are typically

developed using alternative substrates such as sapphire (Al_2O_3), Silicon Carbide (SiC), and silicon (Si) [7]. Nevertheless, owing to its cost effectiveness and availability in large wafer sizes (e.g., 12-inch wafers), Si substrate is widely used and predominant compared to SiC and Al_2O_3 substrates, which are available in smaller-sized wafers (e.g., 6 or 8 inches) [8]. Moreover, silicon technology and fabrication processes are more mature and advanced. Additionally, the presence of an AlGaN (Aluminum Gallium Nitride) modulation layer on silicon substrate plays a crucial role in mitigating defects in GaN semiconductor materials. These factors, along with the higher costs associated with SiC, have positioned silicon as the preferred substrate for electronic industrial production. Although silicon is a dominant choice and more commonly used for electronic applications, it is worth noting that there are specific applications where SiC or sapphire substrates might be preferred, depending on the performance requirements and specific characteristics of the devices being developed.

The packaging of electronic devices plays a critical role in ensuring their functionality, reliability, and protection from external factors (chemicals, light exposure, and mechanical impact) [9] while simultaneously guaranteeing a good connection between the chip and the board. For these reasons, many studies have been conducted to identify the best kind of packaging for the desired applications, testing different designs and materials. More specifically, the electronic device packaging research field has become increasingly active as the demand for power devices has increased [10]. Among all the analyzed factors that can affect both performance and lifetime of a device, the effect of the mechanical stress on the chip surface is rarely taken into account [11]. Due to the lattice mismatch between the AlGaN/GaN HEMT and the chosen substrate, along with the difference in thermal expansion coefficients [12], there is a significant built-in strain/stress capable of modifying the overall performance of GaN-based devices. Moreover, regardless of the type of substrate used, AlGaN/GaN HEMTs must be encapsulated within specific packaging. Minimizing the stress and strain experienced by the devices has been one of the main goals of the research on new packaging materials and designs. Typically, stress and strain can be induced mechanically and thermally; therefore, for different kinds of device, different materials have to be employed. For instance, polymer-based packaging materials provide flexibility and shock absorption, while ceramics offer high stiffness and thermal stability. Furthermore, the overall effect on the device lifetime and performances induced by the packaging is not predictable since there are many elements that constitute the packaging (e.g., wires, solders, die, etc. [13]).

In this work, we studied a commercial electronic device produced by STMicroelectronics equipped with a wire-bonding-free packaging designed to be integrated around the chip to save space and optimize thermal dissipation. The investigation proposed in the manuscript emphasizes the importance of choosing and designing the appropriate packaging to ensure performance and lifetime suitable for the device's mission profile. The proposed package comprises a lead frame onto which the die is soldered using a silver sinter paste. Fiberglass is used to plane the intermediate space. Holes are then dug into the glass fiber, onto which copper is deposited, and subsequently etched down using a dedicated mask, leaving the final connection. Despite its utility, the packaging encapsulation process may induce unwanted additional mechanical residual stresses across various layers of the device and at the die/packaging interface. The additional mechanical stress can be even more burdensome under normal operating conditions due to differences in thermal expansion coefficients between the various materials composing the device [14]. The above results in a continuous stream of reliability challenges in the field of advanced packaging technology. This work focuses on the effect of packaging on the stress among the semiconductor layers constituting the device. In particular, the thermomechanical stress contributes to premature device failure through a variety of mechanisms, including packaging, die, wire, and solder bump crack mechanisms, as well as delamination. The study of the aging effect and failure mechanism caused by thermal and thermomechanical phenomena on electronic devices is currently an active research field [11,15]; therefore, the evaluation of the built-in stress and strain is mandatory to correctly estimate the device

lifetime. To explore this issue, many non-destructive approaches have been employed to measure mechanical strain and stress (e.g., X-Ray Diffraction, Photoluminescence, and Terahertz Time-Domain Spectroscopy [9]). In this context, micro-Raman spectroscopy emerges as a potent non-contact, local, and non-destructive molecular characterization technique [16] capable of assessing localized residual strain/stress across the entire thickness of the AlGaN/GaN HEMT [17] with a sub-micron lateral resolution. Significantly, when crystals are subjected to mechanical stress, the frequency of their characteristic Raman modes shifts due to stress-induced crystal deformations [9]. The GaN crystal Raman spectrum can be populated by eight different optical modes, four of which are Raman active in our geometry, namely A1(TO), E1(TO), E2(low), and E2(high) [18]. Among the detectable phonon modes, the E2(high), which arises from atomic oscillations along the c-plane, is more susceptible to lattice strain elongations, constituting a good marker for the quantification of residual stresses in AlGaN/GaN HEMT devices [19]. According to the previous consideration, the frequency center (ω) of the E2(high) mode was monitored along a vertical direction spanning from the bottom to the top of the HEMT devices, crossing the entire AlGaN/GaN heterostructures. This comprehensive analysis was conducted for both AlGaN/GaN HEMT-PD and AlGaN/GaN HEMT-B samples. This approach, together with using a specific strain/stress relation, enables correlation of the optical data, as achieved by micro-Raman spectroscopy, and the residual stress existing within the layers of the device under test [1,7,20,21]. Knowledge of the aforementioned aspects not only helps evaluation of the performance of GaN-based electronics in various applications, but also provides valuable information for the understanding of the unknown failure mechanisms which compromise their lifetime. The impact of the packaging on the stress of a GaN-based HEMT has never been investigated, but this phenomenon has to be taken into account to design the packaging of high-performance devices. In Table 1, for ease of reading, a list of all the symbols and notations used hereafter is provided.

Table 1. List of symbols and notations used in this paper.

Symbols and Acronyms	Description
MOSFET	Metal–Oxide–Semiconductor Field Effect Transistor
HEMT	High-electron-mobility transistor
HEMT-B	Bare HEMT
HEMT-PD	Packaged HEMT
WBS	Wide-Bandgap Semiconductors
2-DEG	Two-dimensional electron gas
RT	Room temperature
MOCVD	Metal–Organic Chemical Vapor Deposition
SEM	Scanning Electron Microscopy
DPSS	Diode-Pumped Solid State
CCD	Charge-Coupled Device
ω	Measured frequency center of the E2(high) Raman peak
ω_0	Stress-free frequency center of the E2(high) Raman peak
$\Delta\omega$	Frequency shift of the E2(high) Raman peak
σ	Residual stress
K	Stress coefficient

2. Materials and Methods

2.1. Material

In this study, we explore the impact of packaging on local stress through a comparative analysis of the Raman spectral characteristics of the packaged (PD) AlGaN/GaN HEMT and its unpackaged counterpart, the bare (B) AlGaN/GaN HEMT, both provided by STMicroelectronics S.r.l. (Catania, Italy). Figure 1 displays images of both the bare AlGaN/GaN HEMT (a) and its packaged counterpart (b).

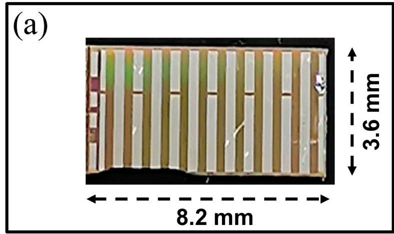

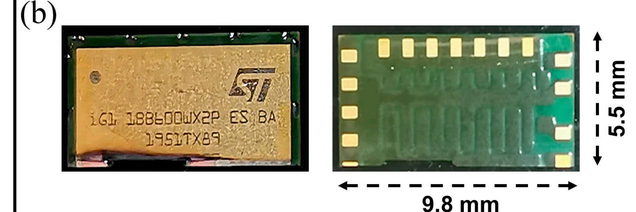

Figure 1. Photographs of the AlGaN/GaN HEMT-B (**a**) and AlGaN/GaN HEMT-PD (**b**).

AlGaN/GaN HEMTs are manufactured by STMicroelectronics S.r.l. by means of Metal–Organic Chemical Vapor Deposition (MOCVD). The process begins with the growth of a 5 µm thick GaN(0001) layer on an n-Si(111) substrate, followed by a 16 nm $Al_{0.25}Ga_{0.75}N$ barrier. Afterwards, a p-GaN capping layer is added on the gate region and then the metallic contacts are deposited. Subsequently, a SiO_2 passivation layer is deposited to ensure electrical isolation for the AlGaN/GaN high-electron-mobility transistors and, ultimately, the packaging. Figure 2 illustrates a cross-sectional view of the AlGaN/GaN HEMT structure.

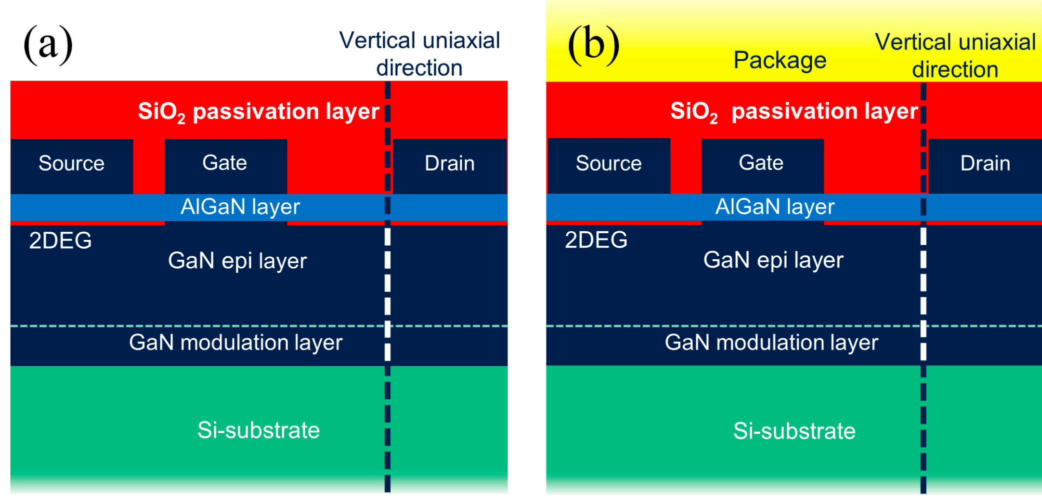

Figure 2. Schematic representation of the internal structure of AlGaN/GaN HEMT-B (**a**) and AlGaN/GaN HEMT-PD (**b**) investigated in this study (not to scale). The vertical dashed line indicates the uniaxial direction along which micro-Raman measurements were performed.

As displayed in Figure 2, the GaN layer can be split in two layers. The first one, with a thickness of roughly 2 µm, acts as a strain modulation layer at the GaN/Si interface, minimizing the lattice mismatch between the two semiconductors. In this way, the GaN epitaxial layer will experience a lower built-in mechanical stress. The employment of the p-GaN cap gate and the equilibrium between the aluminum molar fraction and the thickness of the AlGaN layer achieve normally off HEMTs with a reasonably positive threshold voltage [22]. Moreover, the two-dimensional electron gas (2-DEG) sheet at the GaN epitaxy/AlGaN interface results in efficient charge depletion processes. Two identical devices were prepared; one device was at wafer level (HEMT-B) while the second was encapsulated (HEMT-PD). The purpose was to analyze their Raman spectra and highlight the impact of encapsulation on residual stress.

To acquire the Raman spectra of the device layers, it was necessary to cut it transversely. However, a simple cut and subsequent mechanical polishing are not suitable experimental strategies as the resulting surface roughness would be very high, adding noticeable additional stress to the layers and leading to imprecise measurements. For this reason, an ion beam milling technique was employed on both samples under the same milling conditions. The ion milling procedure involves amorphization of the semiconduc-

tor's surface layers; thus, in principle, the Raman spectrum could be influenced by the cleaning treatment. However, this would only result in a slight peak broadening without significantly affecting its position since the Raman scattering volume and the focal depth of the objective lens ensure that, with proper focusing, most of the Raman signal originates from the deeper layers of the material [23–25]. To attest the quality of the growth and the absence of defect or phase transformations induced by ion milling, a SEM analysis was performed on a milled HEMT-PD device with a beam energy of 5 keV. Figure 3a shows the cross-sectional view of the HEMT-PD device after ion milling, while Figure 3b offers a magnified view of the red-framed area in Figure 3a, which corresponds to the region where the stress distribution was studied. The structure of the device across all layers is clearly visible, with each layer identified and labeled in both Figure 3a,b.

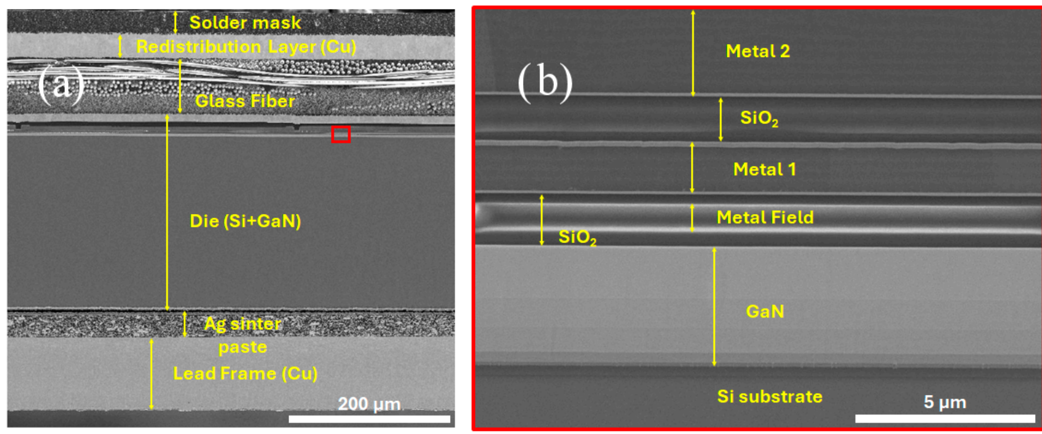

Figure 3. (**a**) SEM image of the cross-sectional view of the device as obtained after ion milling, (**b**) the result of the SEM zoom measurement obtained from the region contained within the red square in image (**a**). The different layers composing the device are clearly visible and identified.

2.2. Method

Micro-Raman spectra were collected along the cross-sections of both HEMT-B and HEMT-PD samples to assess the spectral changes induced by the residual stress [26] across the layers of the devices under test. Measurements were carried out at room temperature (RT) using an NT-MDT NTEGRA Spectra confocal micro-Raman system working in reflection mode. The system is based on a MS3504i spectrometer provided by SOL Instruments Ltd., Augsburg, Germany, and equipped with a 2400 lines/mm grating blazed at 400 nm. A 30 mW linear polarized DPSS laser operating at 532 nm (Nd:YAG laser mod GLK 3250 T01, LASOS Lasertechnik GmbH, Jena, Germany) was employed as excitation source. A neutral filter was introduced in the laser path to limit the maximum power, impinging the sample surface down to ~400 µW. This precaution is needed to prevent any displacement of the Stokes peak induced by the temperature increasing [27]. An IDUS-401 CCD camera provided by Andor, Oxford Instruments Italia s.r.l., Milan (MI), Italy and cooled with a triple Peltier stage was used as detector. For the purpose of this study, we investigated the spectral range between 500 and 600 cm^{-1} with a resolution well below 1 cm^{-1}. A 100× objective with a working distance of 6 mm and a numerical aperture of 0.75 was used to focalize the laser beam on the surface of the sample with a spot size of ~350 nm. All measurements were carried out in backscattering geometry using the microscope objective to capture the scattered light. The samples were positioned with their cross-section facing upwards, taking advantage of a homemade sample holder set-up, as depicted in Figure 4. In our experiment, the spring exerted no force on the device, and it only kept the sample in its position. For each sample, 128 micro-Raman spectra were collected along the direction orthogonal to the layers' growth with a step size of 78 nm, thus covering a 10 µm path and crossing through the GaN heterostructure (see Figure 2).

Each spectrum was acquired with an exposure time of 30 s, and the entire collection process took 64 min.

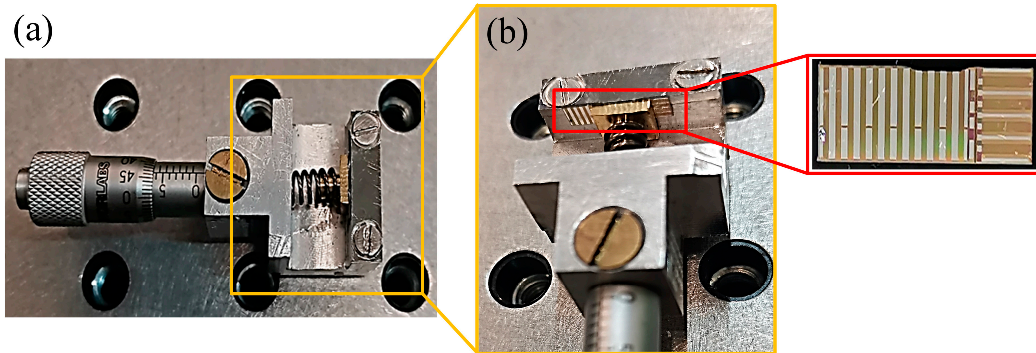

Figure 4. Image of the sample holder (**a**) with details highlighting the sample position (**b**).

3. Results and Discussion

Figure 5a shows an optical microphotograph of the cross-section of the sample on which the study was conducted. In particular, the 128 spectra were acquired along a vertical line crossing the layers (the red line crossing Figure 5a). This strategy allows us to observe how the Raman peaks shift from one layer to another and thus highlights the presence of stress at the interfaces. Since obtaining a sufficient signal-to-noise ratio required integrating the signal for very long time, we chose to proceed with acquiring the Raman spectra along a line instead of performing a full Raman mapping. Indeed, the latter would have required extremely long measurement times, potentially leading to results affected by thermal drift and unpredictable variations in experimental conditions. Moreover, it would not have provided additional useful information to the measurement. Figure 5b shows the 1D map of the Raman spectra acquired during the experiment along the 10 µm investigated (i.e., the Raman intensities acquired point by point plotted against the Raman shift).

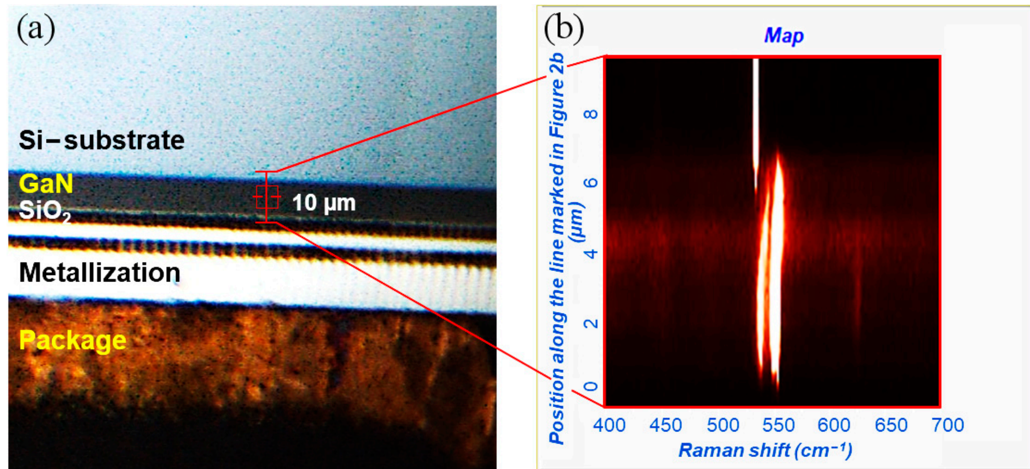

Figure 5. Detailed view of the AlGaN/GaN HEMT-PD heterostructure (**a**) and the resulting Raman map along the 10 µm scanned path (**b**).

It can roughly be said that the spectral structures shift when moving from silicon through the layers of GaN, indicating the presence of intrinsic stress. In particular, the GaN Raman peaks in the lower part of the map start to redshift as the position of the area under analysis approaches the GaN/Si interface. The frequency center of Raman peaks is intimately correlated to the interatomic potential between atoms [28]. Accordingly, changes in this potential due to intrinsic stress within the crystal lead to Raman shifts of specific and characteristic vibrational modes of the structure, regardless of its origin [28].

Figure 6 displays typical micro-Raman spectra acquired at the GaN epitaxy layer (Figure 6a) and at the GaN/Si interface (Figure 6b). The micro-Raman profile collected at the GaN epitaxy layer (Figure 6a) reveals distinct contributions at 531.7 cm^{-1}, 558.7 cm^{-1}, and 567.7 cm^{-1}, respectively, associated to the A1(TO), E1(TO), and E2(high) modes of the hexagonal structure of wurtzite. At the GaN/Si interface (Figure 6b), as expected, a characteristic Si Raman peak centered at 521.4 cm^{-1}, arising from the Si substrate, was clearly distinguished. Furthermore, the Raman mode deriving from GaN structures, E2(high) at 569.6 cm^{-1}, was also observed.

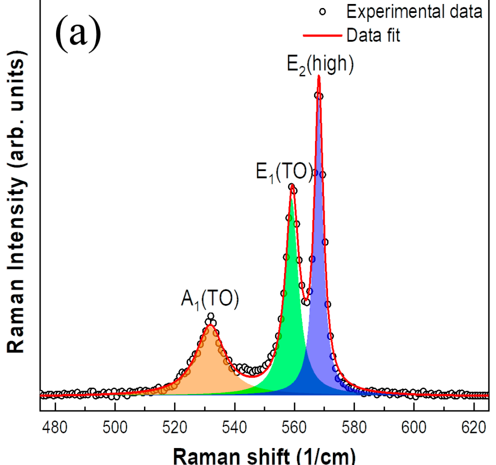

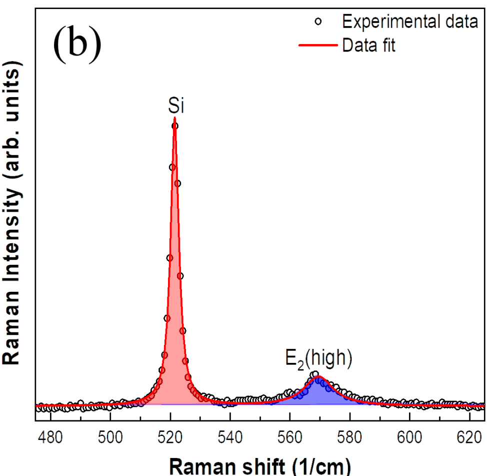

Figure 6. Micro-Raman spectra collected at the GaN epitaxy layer (**a**) and at the GaN/Si interface (**b**) of HEMT-B.

The observed frequency shift of the E2(high) mode, occurring from the GaN epitaxy layer to the GaN/Si interface, can be attributed to the different stress conditions in these two regions.

Since the main purpose of the work was to identify the presence of stress among the layers using Raman spectroscopy, it was necessary to measure the Raman peak positions with the utmost precision. Despite the rather high spectral resolution of the measurement instrument, obtaining accurate information required fitting the experimental data using an appropriate model. In particular, the used model consists of three Lorentzian lines describing the Raman modes of GaN (A1(TO), E1(TO), and E2(high)), and also takes into account the presence of silicon when it needs. All the 128 spectra were fitted using the model described above to obtain the characteristic frequency ω of the modes point by point along the scanned line. Notably, E2(high) mode was found to be particularly sensitive to biaxial stresses compared to both A1(TO) and E1(TO) modes. For this reason, and in agreement with literature, it was used as a marker for quantifying residual stresses [29]. This may be reasonably due to the nature of the E2(high) mode, characterized by atomic oscillations almost perpendicular to the c-axis of wurtzite and hence more sensitive to stress along the chosen axis (see Figure 2).

The inset of Figure 7 shows the trend of the frequency of mode E2(high) in the HEMT-B sample (red line) and HEMT-PD sample (blue line) when moving along the vertical path represented by the red line in Figure 5, i.e., crossing the AlGaN/GaN heterostructure starting from the package side and moving towards the silicon substrate.

The E2(high) ω values allow calculation of the residual stress point by point within the AlGaN/GaN HEMT devices. Indeed, the frequency shift ($\Delta\omega$) linearly depends on the residual stress (σ) according to the relationship:

$$\langle \Delta\omega \rangle = K \langle \sigma \rangle$$

where K represents the stress coefficient, equal to 4.3 cm^{-1}/GPa for GaN grown on c-direction silicon [30]. The frequency shift, $\Delta\omega$, is defined as $\Delta\omega = \omega - \omega_0$, where ω is the peak frequency center, and ω_0 accounts for the corresponding stress-free E2(high) peak frequency center, fixed at 568 cm^{-1} [31]. It should be noted that, even if there was a slight influence on the stress due to the ion milling treatment, this influence would be the same in both samples since the milling conditions were the same. Therefore, $\Delta\omega$ was not affected by the preparation of the samples.

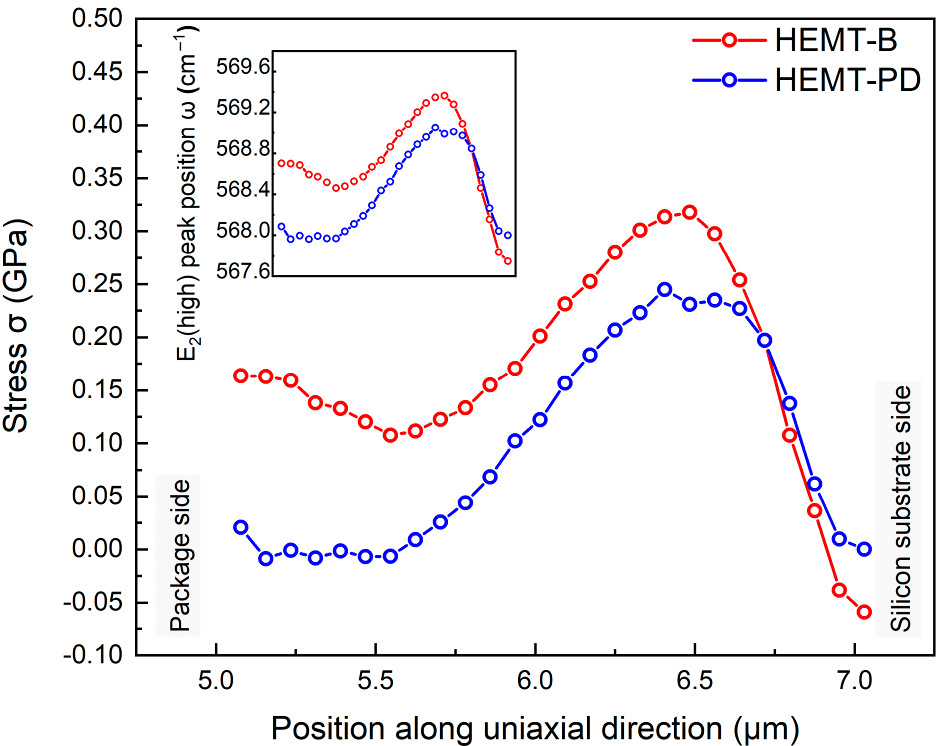

Figure 7. Stress distribution along the uniaxial direction, covering a range from 5 μm to 7 μm within the GaN layer, for both AlGaN/GaN HEMT-B and AlGaN/GaN HEMT-PD devices. The inset graph represents the E2(high) peak frequency center plotted against the position along the uniaxial direction in μm.

Figure 7 shows the residual stress σ in GPa, inferred from the frequency shift E2(high) $\Delta\omega$, as a function of position along the studied path for both HEMT-B (red line) and HEMT-PD (blue line) devices.

Due to the linear correlation between stress and frequency shift, the E2(high) mode frequency center follows a pattern mirroring that of the stress, as can be deduced by observing the inset of Figure 7. Analyzing the residual stress trend along the AlGaN/GaN HEMT structure (Figure 7), it is worth noting that the influence of the package was mainly visible in the range from 5 μm to 6 μm (zone of interest). In the range between 6.55 μm and 7 μm, the lattice mismatch at the GaN/Si interface induced a more pronounced tensile stress compared to that generated by the presence of packaging, as highlighted by the redshift (a shift towards lower frequencies) of the E2(high) mode. Furthermore, the non-monotonic behavior observed can be attributed to both the characteristics of the multilayer structure and/or the doping of the layers composing the device. The behavior of E2(high) in HEMT-B (red curve in the graph shown in Figure 7) showed a slight initial shift towards lower frequency values as it moved through the layers from 5 μm to ~5.5 μm, indicating the presence of tensile stress. This was followed by a clear shift towards the blue in E2(high), attributed to compression stress likely induced by additional forces or applied loads. Subsequently, near the silicon substrate, a noticeable tensile stress was observed, characterized by a frequency shift towards lower frequencies, probably stemming from

the lattice mismatch between the GaN and silicon. The behavior of the E2 mode in the HEMT-PD device was entirely similar. However, the observed stress values were generally lower across the entire device (blue curve in the graph shown in Figure 7).

The influence of packaging was evident only within the specified area of interest (from 5 μm to 6.55 μm) located near the surface of the device. Within this region, the packaged device (HEMT-PD) showed a decrease in stress levels of about 0.1 GPa compared to the bare one (HEMT-B). This stress mitigation was attributed to the compression introduced by the packaging, which compensates for the intrinsic tensile stress present between the layers of the device. This result stems from a proper choice of material and packaging design, which must be optimized in terms of shape, dimensions, and thermal properties. Additionally, the incorporation of intermediate layers or buffer materials with more similar thermal properties contributes to reducing stress at interfaces between different materials and ensures effective stress mitigation across the mold.

The mitigation of stress within the active layers of the device has a direct impact on its reliability and performance. Indeed, thermal-mechanical stresses and deformations are already well-known and extensively studied failure mechanisms. In general, lower stress leads to slower aging of the device. Furthermore, when current flows through a device, it undergoes thermal expansion proportional to the current itself due to the increase in temperature in the active region of the device [11]. Generally, this deformation is not uniform across the entire device but depends on the shape and arrangement of the semiconductor part through which the current flows. Particularly in power switching applications, current values can be very high, resulting in intense heat release and consequent mechanical deformation. Since the crystal can withstand defined stress values beyond which it breaks, it is evident that the presence of residual stress when the device is off can limit the maximum current that can flow through the device without destroying it. This aspect, along with more specifically thermal aspects, must be taken into account when defining the mission profile. Considering the above, residual stress mitigation is, among all other advantages, a potential way to improve the device's performance and increase its lifetime [32,33]. Therefore, we can conclude that proper packaging design can effectively enhance the quality and overall reliability of the devices.

4. Conclusions

In this article, micro-Raman spectroscopy was employed to assess the stress/deformation induced by packaging in AlGaN/GaN high-electron-mobility transistors (HEMTs) supplied by STMicroelectronics S.r.l. To evaluate the packaging's impact, we acquired 128 micro-Raman spectra by vertically scanning along the AlGaN/GaN heterostructure of the device. The data were analyzed using a fitting procedure employing a model consisting of three or four Lorentzians to accurately measure the frequency shift of the phonon modes' center. Attention was focused on the E2(high) phonon mode, which is highly sensitive to crystalline stress and therefore can be effectively used for its quantification. Two GaN devices supplied by STMicroelectronics S.r.l were studied, one packaged and the other bare, to assess the influence of packaging on the residual stress present within the active layers of the device.

In the HEMT-PD device, a blue shift of the E2(high) mode near the packaging was observed, while a slight redshift followed by a blue shift was observed for the bare device. A linear correlation between the Raman frequency shift $\Delta\omega$ and stress σ was used to evaluate the compression stress induced by packaging. The packaged device showed a decrease in stress levels of about 0.1 GPa compared to the bare HEMT. In conclusion, the study states that the compression stress induced by the packaging process strongly mitigates the residual tensile stress present on wafer-level HEMT-B devices. Therefore, packaging, which provides mechanical support and protects the sensitive semiconductor wafer from external environmental factors, can play a dual role by also contributing to stress mitigation, compensating for the inherent tensile stress in these devices, and thereby improving performance in terms of reliability, dynamics, and lifetime.

Author Contributions: Conceptualization, M.C. and S.P.; Methodology, S.P.; Formal analysis, G.M. and M.d.; Investigation, Z.D., A.A.M., M.M. and A.S.; Data curation, Z.D. and M.C.; Writing—original draft, Z.D. and G.M.; Writing—review & editing, M.d., A.A.M., M.M., A.S., M.C. and S.P.; Supervision, S.P.; Funding acquisition, A.A.M. All authors have read and agreed to the published version of the manuscript.

Funding: This work has been carried out in the framework of the European Project GaN4AP (Gallium Nitride for Advanced Power Applications). The project has received funding from the Electronic Component Systems for European Leadership Joint Undertaking (ECSELJU) under grant agreement no. 101007310. This Joint Undertaking received support from the European Union's Horizon 2020 research and innovation programme, and Italy, Germany, France, Poland, Czech Republic, and the Netherlands.

Institutional Review Board Statement: Not applicable.

Informed Consent Statement: Not applicable.

Data Availability Statement: The raw data supporting the conclusions of this article will be made available by the authors on request.

Conflicts of Interest: Authors Giuliana Malta, Angelo Alberto Messina, Mattia Musolino, Alessandro Sitta and Michele Calabretta were employed by the company ST Microelectronics. The remaining authors declare that the research was conducted in the absence of any commercial or financial relationships that could be construed as potential conflicts of interest.

References

1. Zhao, D.G.; Xu, S.J.; Xie, M.H.; Tong, S.Y.; Yang, H. Stress and Its Effect on Optical Properties of GaN Epilayers Grown on Si(111), 6H-SiC(0001), and *c* -Plane Sapphire. *Appl. Phys. Lett.* **2003**, *83*, 677–679. [CrossRef]
2. Ishida, T. GaN HEMT Technologies for Space and Radio Applications. *Microw. J.* **2011**, *54*, 56–66.
3. Trew, R.J.; Bilbro, G.L.; Kuang, W.; Liu, Y.; Yin, H. Microwave AlGaN/GaN HFETs. *IEEE Microw. Mag.* **2005**, *6*, 56–66. [CrossRef]
4. Mishra, U.K.; Parikh, P.; Wu, Y.P. AlGaN/GaN HEMTs—An Overview of Device Operation and Applications. *Proc. IEEE* **2002**, *90*, 1022–1031. [CrossRef]
5. Islam, N.; Mohamed, M.F.P.; Khan, M.F.A.J.; Falina, S.; Kawarada, H.; Syamsul, M. Reliability, Applications and Challenges of GaN HEMT Technology for Modern Power Devices: A Review. *Crystals* **2022**, *12*, 1581. [CrossRef]
6. Cho, J.; Li, Z.; Asheghi, M.; Goodson, K.E. Near-junction thermal management: Thermal conduction in gallium nitride composite substrates. *Annu. Rev. Heat Transf.* **2015**, *18*, 7–45. [CrossRef]
7. Liu, L.; Edgar, J.H. Substrates for Gallium Nitride Epitaxy. *Mater. Sci. Eng. R Rep.* **2002**, *37*, 61–127. [CrossRef]
8. Schuster, M.; Wachowiak, A.; Szabo, N.; Jahn, A.; Merkel, U.; Ruf, A.; Mikolajick, T.; Murad, S.; Hu, C.; Groh, L.; et al. HEMT Test Structure Technology for Fast On-Wafer Characterization of Epitaxial GaN-on-Si Material. In Proceedings of the 2013 International Semiconductor Conference Dresden—Grenoble (ISCDG), Dresden, Germany, 26–27 September 2013; pp. 1–3.
9. Ma, L.; Qiu, W.; Fan, X. Stress/Strain Characterization in Electronic Packaging by Micro-Raman Spectroscopy: A Review. *Microelectron. Reliab.* **2021**, *118*, 114045. [CrossRef]
10. Bayerer, R. Advanced Packaging Yields Higher Performance and Reliability in Power Electronics. *Microelectron. Reliab.* **2010**, *50*, 1715–1719. [CrossRef]
11. Panarello, S.; Garesci, F.; Triolo, C.; Patane, S.; Patti, D.; Russo, S. Reliability Model Application for Power Devices Using Mechanical Strain Real Time Mapping. In Proceedings of the 2016 28th International Symposium on Power Semiconductor Devices and ICs (ISPSD), Prague, Czech Republic, 12–16 June 2016; pp. 127–130.
12. Kim, Y.; Subramanya, S.G.; Siegle, H.; Krüger, J.; Perlin, P.; Weber, E.R.; Ruvimov, S.; Liliental-Weber, Z. GaN Thin Films by Growth on Ga-Rich GaN Buffer Layers. *J. Appl. Phys.* **2000**, *88*, 6032–6036. [CrossRef]
13. Lu, D.; Wong, C.P. (Eds.) *Materials for Advanced Packaging*; Springer: Boston, MA, USA, 2009; ISBN 978-0-387-78218-8.
14. Ahmad, I.; Holtz, M.; Faleev, N.N.; Temkin, H. Dependence of the Stress–Temperature Coefficient on Dislocation Density in Epitaxial GaN Grown on α-Al_2O_3 and 6H–SiC Substrates. *J. Appl. Phys.* **2004**, *95*, 1692–1697. [CrossRef]
15. Testa, A.; De Caro, S.; Panarello, S.; Patane, S.; Letor, R.; Russo, S.; Poma, S.; Patti, D. Stress Analysis and Lifetime Estimation on Power MOSFETs for Automotive ABS Systems. In Proceedings of the 2008 IEEE Power Electronics Specialists Conference, Rhodes, Greece, 15–19 June 2008; pp. 1169–1175.
16. Xu, Z.; He, Z.; Song, Y.; Fu, X.; Rommel, M.; Luo, X.; Hartmaier, A.; Zhang, J.; Fang, F. Topic Review: Application of Raman Spectroscopy Characterization in Micro/Nano-Machining. *Micromachines* **2018**, *9*, 361. [CrossRef]
17. Choi, S.; Heller, E.; Dorsey, D.; Vetury, R.; Graham, S. Analysis of the Residual Stress Distribution in AlGaN/GaN High Electron Mobility Transistors. *J. Appl. Phys.* **2013**, *113*, 093510. [CrossRef]
18. Kamarudzaman, A.; Abu Bakar, A.S.B.; Azman, A.; Omar, A.-Z.; Supangat, A.; Talik, N.A. Positioning of Periodic AlN/GaN Multilayers: Effect on Crystalline Quality of a-Plane GaN. *Mater. Sci. Semicond. Process.* **2020**, *105*, 104700. [CrossRef]

19. Maize, K.; Pavlidis, G.; Heller, E.; Yates, L.; Kendig, D.; Graham, S.; Shakouri, A. High Resolution Thermal Characterization and Simulation of Power AlGaN/GaN HEMTs Using Micro-Raman Thermography and 800 Picosecond Transient Thermoreflectance Imaging. In Proceedings of the 2014 IEEE Compound Semiconductor Integrated Circuit Symposium (CSICS), La Jolla, CA, USA, 19–22 October 2014; pp. 1–8.
20. Rieger, W.; Metzger, T.; Angerer, H.; Dimitrov, R.; Ambacher, O.; Stutzmann, M. Influence of Substrate-Induced Biaxial Compressive Stress on the Optical Properties of Thin GaN Films. *Appl. Phys. Lett.* **1996**, *68*, 970–972. [CrossRef]
21. Kisielowski, C.; Krüger, J.; Ruvimov, S.; Suski, T.; Ager, J.W.; Jones, E.; Liliental-Weber, Z.; Rubin, M.; Weber, E.R.; Bremser, M.D.; et al. Strain-Related Phenomena in GaN Thin Films. *Phys. Rev. B* **1996**, *54*, 17745–17753. [CrossRef]
22. Greco, G.; Iucolano, F.; Roccaforte, F. Review of Technology for Normally-Off HEMTs with p-GaN Gate. *Mater. Sci. Semicond. Process.* **2018**, *78*, 96–106. [CrossRef]
23. Myers, K.E.; Walls, D.J.; Wilker, C.; Pang, P.S.W.; Carter, C.F. Raman Microprobe Analysis of Patterned Tl-2212 Thin Films. *IEEE Trans. Appl. Supercond.* **1997**, *7*, 2126–2129. [CrossRef]
24. Wang, X.H.; Ning, J.Q.; Xu, S.J.; Choi, H.W. Raman and Photoluminescence Characterization of Focused Ion Beam Patterned InGaN/GaN Multi-Quantum-Wells Nanopillar Array. *J. Appl. Phys.* **2011**, *110*, 093111. [CrossRef]
25. Mishra, P.; Janjua, B.; Ng, T.K.; Anjum, D.H.; Elafandy, R.T.; Prabaswara, A.; Shen, C.; Salhi, A.; Alyamani, A.Y.; El-Desouki, M.M.; et al. On the Optical and Microstrain Analysis of Graded InGaN/GaN MQWs Based on Plasma Assisted Molecular Beam Epitaxy. *Opt. Mater. Express* **2016**, *6*, 2052. [CrossRef]
26. Beechem, T.; Christensen, A.; Green, D.S.; Graham, S. Assessment of Stress Contributions in GaN High Electron Mobility Transistors of Differing Substrates Using Raman Spectroscopy. *J. Appl. Phys.* **2009**, *106*, 114509. [CrossRef]
27. Choi, S.; Heller, E.R.; Dorsey, D.; Vetury, R.; Graham, S. Thermometry of AlGaN/GaN HEMTs Using Multispectral Raman Features. *IEEE Trans. Electron. Devices* **2013**, *60*, 1898–1904. [CrossRef]
28. Beechem, T.E.I. *Metrology of Gan Electronics Using Micro-Raman Spectroscopy*; Georgia Institute of Technology: Atlanta, GA, USA, 2008.
29. Sugie, R.; Uchida, T. Determination of Stress Components in 4H-SiC Power Devices via Raman Spectroscopy. *J. Appl. Phys.* **2017**, *122*, 195703. [CrossRef]
30. Tripathy, S.; Chua, S.J.; Chen, P.; Miao, Z.L. Micro-Raman Investigation of Strain in GaN and AlxGa1−xN/GaN Heterostructures Grown on Si(111). *J. Appl. Phys.* **2002**, *92*, 3503–3510. [CrossRef]
31. Harima, H. Properties of GaN and Related Compounds Studied by Means of Raman Scattering. *J. Phys. Condens. Matter* **2002**, *14*, R967–R993. [CrossRef]
32. Osipov, K.Y.; Ostermay, I.; Brunner, F.; Wurfl, J.; Trankle, G. Effect of External Mechanical Stress on DC Performance and Reliability of Integrated E/D GaN HEMTs. *IEEE Trans. Semicond. Manuf.* **2018**, *31*, 419–425. [CrossRef]
33. Choi, S.; Heller, E.; Dorsey, D.; Vetury, R.; Graham, S. The Impact of Mechanical Stress on the Degradation of AlGaN/GaN High Electron Mobility Transistors. *J. Appl. Phys.* **2013**, *114*, 164501. [CrossRef]

Disclaimer/Publisher's Note: The statements, opinions and data contained in all publications are solely those of the individual author(s) and contributor(s) and not of MDPI and/or the editor(s). MDPI and/or the editor(s) disclaim responsibility for any injury to people or property resulting from any ideas, methods, instructions or products referred to in the content.